Photolysis of Hexafluoroacetone in the Presence of H2, D2, and HD. Kinetic Isotope Effects in the Reaction of CF3 with Molecular Hydrogen

Charles L. Kibby and Ralph E. Weston Jr.

Citation: The Journal of Chemical Physics **49**, 4825 (1968); doi: 10.1063/1.1669966
View online: http://dx.doi.org/10.1063/1.1669966
View Table of Contents: http://scitation.aip.org/content/aip/journal/jcp/49/11?ver=pdfcov
Published by the AIP Publishing

Photolysis of Hexafluoroacetone in the Presence of H_2, D_2, and HD. Kinetic Isotope Effects in the Reaction of CF_3 with Molecular Hydrogen*

CHARLES L. KIBBY† AND RALPH E. WESTON, JR.
Chemistry Department, Brookhaven National Laboratory, Upton, New York 11973

(Received 30 July 1968)

The photolysis of hexafluoroacetone has been used as a source of CF_3 radicals which either react with hydrogen to produce fluoroform or recombine to form hexafluoroethane. Relative rates of these reactions approximately obey the Arrhenius expressions over the temperature range from 333° to 870°K,

$$k_{H_2}/2k_2^{1/2} = 9.3\times10^{8} \exp[(-10\,660\pm140)/RT] \text{ liter}^{1/2}\,\text{mole}^{-1/2}\cdot\text{sec}^{-1/2},$$

$$k_{HD}/k_2^{1/2} = 7.4\times10^{8} \exp[(-10\,770\pm150)/RT],$$

$$k_{DH}/k_2^{1/2} = 9.6\times10^{8} \exp[(-11\,630\pm130)/RT],$$

$$k_{D_2}/2k_2^{1/2} = 6.9\times10^{8} \exp[(-11\,660\pm110)/RT].$$

Direct measurements of isotope effects were obtained by mass spectrometric analysis of the fluoroform produced during photolysis with added H_2/D_2 mixtures or with HD. Rate constant ratios are $k_{H_2}/k_{D_2} = 1.30\exp(1050/RT)$, $k_{HD}/k_{DH} = 0.78\exp(860/RT)$. The observed isotope effects are compared with those calculated on the basis of three- and six-atom LEPS and BEBO models for the activated complex.

I. INTRODUCTION

A number of kinetic isotope effects in gas-phase reactions have been measured for the purpose of learning about the potential-energy surfaces of the reacting systems. These include triatomic systems such as H_2+Cl,[1,2] and more complex systems such as CF_3+CH_4,[3] or $Cl+CH_4$.[4] We report here the kinetic isotope effects for reactions of the trifluoromethyl radical with hydrogen isotopes, and a comparison of the measurements with isotope effects predicted on the basis of empirical and semiempirical transition-state models. A large number of rate constant measurements have also been made and are discussed in some detail. These reactions have been previously studied[5,6]; however, our work is an extension of the temperature range and an improvement in isotopic analysis.

II. EXPERIMENTAL

A. Materials

After hexafluoroacetone (Allied Chemical) had been degassed under vacuum, the only impurity detected by infrared spectroscopy or by gas chromatography on a squalane column was the hydrate. The hydrate was removed by fractional distillation *in vacuo*. The infrared spectrum of the purified acetone was in good agreement with that reported by Berney,[7] and the vapor pressure was identical with that reported by the manufacturer.[8] The hexafluoroacetone was stored at room temperature in a light-shielded vessel; no decomposition occurred over a period of one year.

A sample of HD was provided by Dr. D. R. Christman of this Laboratory. Mass spectrometer analysis showed its composition to be 1.2% H_2, 97.7% HD, and 1.0% D_2. It was later found to contain a trace ($\leq$0.04%) of methane; corrections for this impurity were negligible. Deuterium was obtained from Stuart Oxygen Company and analysis of this gas showed that it contained 1.2% HD. Prepurified hydrogen was obtained from Matheson Company. Pure samples of CF_4, C_3F_8, CF_3H, and CO from Matheson Company, C_2F_6 from Peninsular Chem Research, and CF_3D from Merck, Sharp, and Dohme were used for gas chromatograph and mass spectrometer calibrations.

B. Apparatus

A conventional vacuum line capable of evacuation to 10^{-5} torr was used to handle reactant and product gases. Product fractions, initially separated by two LeRoy stills in series, were collected and measured in calibrated volumes by means of a Toepler pump fitted with a reference manometer. Pressure measurements were made with McLeod gauges or with a mercury manometer and Wild cathetometer which could be read to 0.01 torr. Temperatures were measured in the photolysis cell with chromel–alumel thermocouples calibrated for the temperature range used, and in the LeRoy stills with copper–constantan thermocouples.

A cylindrical quartz photolysis cell, 63 mm in

* This research sponsored by the U.S. Atomic Energy Commission.

† Present address: Mellon Institute, Pittsburgh, Pa. 15213.

[1] A. Persky and F. S. Klein, J. Chem. Phys. **44**, 3617 (1966).

[2] J. Bigeleisen, F. S. Klein, R. E. Weston, and M. Wolfsberg, J. Chem. Phys. **30**, 1340 (1959).

[3] T. E. Sharp and H. S. Johnston, J. Chem. Phys. **37**, 1541 (1962); H. S. Johnston and E. Tschuikow-Roux, *ibid.* **36**, 463 (1962).

[4] G. Chiltz, R. Eckling, R. Goldfinger, G. Huybrechts, H. S. Johnston, L. Meyers, and G. Verbeke, J. Chem. Phys. **38**, 1053 (1963); K. B. Wiberg and E. L. Motell, Tetrahedron **19**, 2009 (1963).

[5] G. O. Pritchard, H. O. Pritchard, H. I. Schiff, and A. F. Trotman-Dickenson, Trans. Faraday Soc. **52**, 849 (1956).

[6] P. B. Ayscough and J. C. Polanyi, Trans. Faraday Soc. **52**, 960 (1956).

[7] C. V. Berney, Spectrochim. Acta **21**, 1809 (1965).

[8] Allied Chemical Product Data Sheet PD-56FK-663.

diameter, with a volume of 225 cc and a 10-cm light path, was housed in a well-insulated air bath furnace, and fitted with a thermocouple well and filling tube. The furnace was heated with three windings of Nichrome wire around a central ceramic thimble, open at one end, which contained the photolysis cell. The filling tube passed through a small hole in the other end of the ceramic thimble and was attached to the vacuum manifold with a grease-free Kern diaphragm valve, or later with a Teflon needle valve seated with an O ring. The dead volume outside the furnace was 3–4 cc with the Kern valve, but only 0.5 cc when the needle valve was installed. Thermocouples on the outside of the cell indicated a temperature uniformity of $\pm 1°C$; the reported temperatures are from readings taken with the thermocouple junction at the center of the cell. Initially the temperature of the furnace was controlled to $\pm 1°C$ during a run by regulating the power input to the heating coils with Variacs. Later a Radio Frequency Labs Model 55 controller was installed; this maintained the temperature constant to $\pm 0.2°C$. Light from a Hanovia medium-pressure mercury lamp passed through a Corning 9700 filter, which absorbs 2537-Å radiation, so that the radiation absorbed by the acetone was primarily from the 3130-Å line. A quartz lens partially collimated the light and provided total illumination of the cell through a double quartz window (two 1-mm plates separated by a 1-in. air space) at the open end of the ceramic thimble in the furnace.

Complete separation and analysis of product fractions was carried out on an Aerograph Model 204 dual-column gas chromatograph, equipped with a Gow-Mac 301 microvolume thermal conductivity detector. Separations of C_2F_6, C_3F_8, CF_3H, and C_2F_5H were made on a stainless-steel column (10 ft long, $\frac{1}{8}$-in. diameter) packed with activated alumina; H_2, CO, and CH_4 separations were done on a similar column packed with a 5-Å molecular sieve. Column temperatures were 100° and 65°C, respectively, with helium flowing at a rate of 15–20 ml/min as the carrier gas. Detector conditions of 85°C and a current of 195 mA were maintained as constant as possible both for calibrations and product analyses. Relative compositions of product fractions were determined by peak area measurements. The peak area/mole ratios were linear over the concentration range found for each of the components; absolute values were reproducible to $\pm 2\%$ while relative compositions were reproducible to $\pm 0.3\%$. Provision was made to trap the effluent peaks for later mass spectrometer analysis. It was found that the fluoroform peak could be trapped quantitatively with no change in the CF_3H:CF_3D ratio between the original sample and the trapped sample.

Isotopic analyses of H_2, HD, D_2, and CF_3H–CF_3D mixtures were made on a CEC 21-201 Isotope Ratio mass spectrometer. The isotope ratio provision was not used, but rather the mass peaks were scanned in the usual manner by varying the magnetic field at a constant accelerating voltage (1000 V) for CF_3H–CF_3D, and by changing the voltage at constant magnetic field for H_2, HD, and D_2. Whenever possible, the same inlet pressures and leak openings were used. For some analyses of CF_3H–CF_3D the quantities were too small for this to be done; however, no noticeable errors were introduced in these cases, except that the precision was lowered. The isotopic composition of CF_3H–CF_3D mixtures could be accurately determined by a comparison of the peaks corresponding to $m/e=51$ (CF_2H^+) and to $m/e=52$ (CF_2D^+) after correction for ^{13}C; analyses of a given sample were reproducible to $\pm 0.3\%$.

C. Experimental Procedures

Hexafluoroacetone and an appropriate mixture of hydrogen isotopes were mixed and admitted to the photolysis cell at the desired temperature. The quantity of each component was determined by pressure and temperature measurements in calibrated volumes. After a 15-min warm-up period the light from the Hanovia lamp was admitted to the cell for a timed interval, and the product mixture was then passed into the LeRoy stills cooled to $-196°C$. Noncondensable gases (H_2 and CO) were pumped off and collected for later analysis. A second fraction was then taken with the first still at $-100°C$ (above the melting point of hexafluoroacetone) and the second still at $-140°C$. This fraction, containing C_2F_6, C_3F_8, CF_3H, and C_2F_5H, was condensed into a transfer cell for gas chromatographic analysis. A third fraction, consisting mainly of unreacted hexafluoroacetone, was taken by allowing the stills to warm up to room temperature. The pressure, volume, and temperature of each fraction were measured. The first fraction was analyzed on the gas chromatograph for CO content. After many runs showed that the product ratio $2CO/CF_3$ was always unity within experimental error, this ratio was no longer measured. The second fraction was also analyzed on the gas chromatograph; for runs in which both CF_3H and CF_3D were formed the effluent fluoroform was trapped, and its isotopic composition was determined on the mass spectrometer. The third fraction was also analyzed on the gas chromatograph for a few runs. Hexafluoroacetone did not pass through the alumina column, but did pass through a squalane column. Separation with the LeRoy still was adequate since no C_2F_6, CF_3H, or C_3F_8 was left in the third fraction. One or two minor components were found; this is discussed below.

III. RESULTS

The photolytic decomposition, fluorescence, and phosphorescence of hexafluoroacetone have been well studied.[9] There is evidence that CF_3CO radicals may be

[9] R. K. Boyd, G. B. Carter, and K. O. Kutschke, Can. J. Chem. **46**, 175 (1968); earlier references are cited herein.

formed in the primary decomposition step,[10] but in the absence of an efficient scavenger for these radicals a rapid decomposition to yield carbon monoxide and two trifluoromethyl radicals occurs.

$$CF_3COCF_3 \xrightarrow[h\nu]{k_0} 2CF_3 + CO. \qquad (1)$$

In the presence of hydrogen, no evidence for reactions of CF_3CO radicals was found in these experiments, and the product balance ($\sum CF_3 = 2CO$) was quite good. Therefore the production of CF_3 is adequately represented by Eq. (1). The low extinction coefficient at 3130 Å ($6.8M^{-1}\,cm^{-1}$), low concentrations of CF_3COCF_3 ($\sim 5\times10^{-4}M$), and low conversions (5%–10%) ensured a first-order rate of disappearance of CF_3COCF_3:

$$d(CF_3COCF)/dt = k_0(CF_3COCF_3).$$

The value of k_0 depends on temperature, pressure, and wavelength since there is collisional deactivation of the excited CF_3COCF_3 as well as fluorescence and phosphorescence. Three runs at a constant temperature of 376°K, at 3130 Å, and with concentrations of CF_3COCF_3 between $4\times10^{-5}M$ and $13\times10^{-5}M$ yielded $k_0 = 1.28\pm 0.02\times10^{-5}$ sec^{-1}, so that the light intensity was quite steady and reproducible. At this temperature the quantum yield is less than unity; experiments at a temperature of 500°K where the quantum yield is nearly unity gave $k_0 = 1.65\times10^{-5}$ sec^{-1}, and an estimated light flux of 1.6×10^{16} quanta/sec entering the cell at an effective wavelength of 3130 Å. The value of k_0 increases to approximately 5×10^{-5} sec^{-1} at 600°K. Since thermal decomposition was negligible at these temperatures the quantum yield must be greater than unity at this temperature.

The trifluoromethyl radicals formed may recombine, add to the acetone, or abstract hydrogen atoms from a suitable substrate. The recombination rate was found to be second order for the range of pressures and temperatures used; therefore, this reaction is well represented by

$$2CF_3 \xrightarrow{k_2} C_2F_6. \qquad (2)$$

With the hydrogen isotopes, the abstraction reactions are

$$CF_3 + H_2 \xrightarrow{k_{H_2}} CF_3H + H, \qquad (3)$$

$$CF_3 + HD \xrightarrow{k_{HD}} CF_3H + D, \qquad (4)$$

$$CF_3 + HD \xrightarrow{k_{DH}} CF_3D + H, \qquad (5)$$

$$CF_3 + D_2 \xrightarrow{k_{D_2}} CF_3D + D. \qquad (6)$$

[10] B. G. Tucker and E. Whittle, Trans. Faraday Soc. **61**, 484 (1965); J. S. E. McIntosh and G. B. Porter, *ibid.* **64**, 119 (1968).

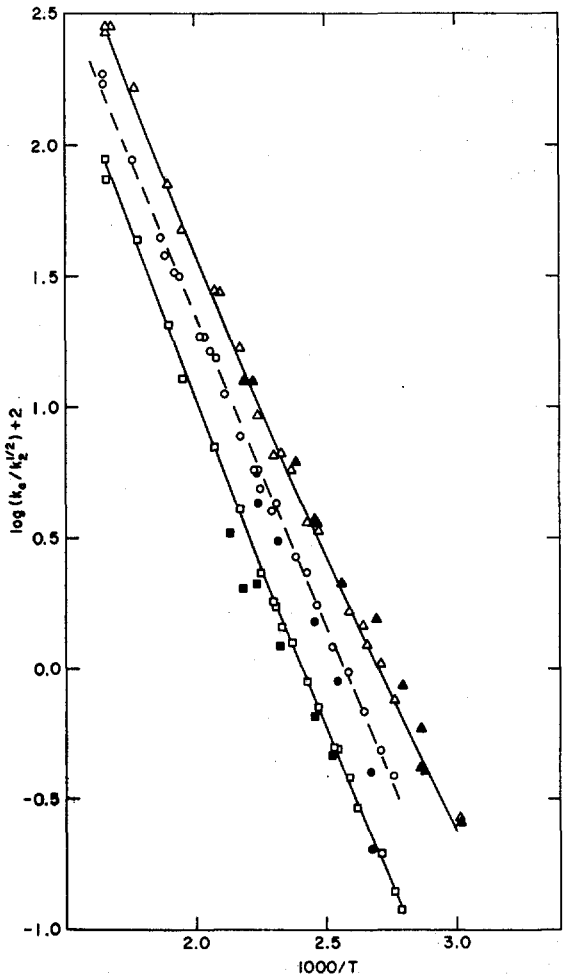

FIG. 1. Ratios of rate constants for abstraction relative to radical recombination as a function of temperature. Rate constant ratio in units of liter$^{1/2}$ mole$^{-1/2}$·sec$^{-1/2}$. Triangles, reaction with H_2; Circles, reaction with HD; Squares, reaction with D_2. Open points are for this work, while closed points are from Ref. 6. Solid lines are calculated from three-parameter expressions, dashed line from the Arrhenius equation (parameters from Tables IV and V).

The addition reaction was found to be relatively minor, so that Reactions (2)–(6) represent the major fate of the trifluoromethyl radicals produced, and are fast enough so that stationary-state conditions are established, and

$$d(CF_3)/dt \approx 0.$$

It is shown below that the majority of hydrogen atoms formed in Reactions (3)–(6) disappear by surface recombination, in a process first order with respect to the hydrogen atom concentration. Hence,

$$k_{wall}(H) = 2k_{H_2}(CF_3)(H_2) \qquad (A)$$

and

$$-d(H_2)/dt = \tfrac{1}{2}k_{H_2}(CF_3)(H_2) \qquad (B)$$

so that the rate of disappearance of H_2 is also first order.

Under conditions of steady illumination, the rate constants for abstraction and recombination cannot be

separated. One obtains only the appropriate ratio of these constants:

$$k_{H_2}/k_2^{1/2}=\text{rate}(CF_3H)/[\text{rate}(C_2F_6)]^{1/2}(H_2). \quad (C)$$

Under stationary-state conditions and with only H_2 added to CF_3COCF_3, this ratio is given by

$$k_{H_2}/k_2^{1/2}=\frac{-2\ln\{1-[(CF_3H)_t/2(H_2)_0]\}}{(C_2F_6)_t^{1/2}t^{1/2}}. \quad (D)$$

In this expression t is the photolysis time, and the subscripts t and 0 designate concentrations at time t and the starting time, respectively. In most experiments about 1% of the hydrogen reacted; in such cases an excellent approximation to Eq. (D) is given by

$$k_{H_2}/k_2^{1/2}=(CF_3H)_t/(C_2F_6)_t^{1/2}(H_2)_{Av}t^{1/2}, \quad (E)$$

where $(H_2)_{Av}=[(H_2)_0+(H_2)_t]/2$.

For runs with more than one isotopic species of hydrogen present,

$$d(CF_3H)/dt=k_{H_2}(CF_3)(H_2)+k_{HD}(CF_3)(HD)$$

and

$$d(CF_3D)/dt=k_{D_2}(CF_3)(D_2)+k_{DH}(CF_3)(DH).$$

Then the following approximate equations, valid for low conversions, may be used:

$$k_{H_2}/k_2^{1/2}=[(CF_3H)_t/(C_2F_6)_t^{1/2}t^{1/2}(H_2)_{Av}]-[k_{HD}(HD)_{Av}/k_2^{1/2}(H_2)_{Av}], \quad (F)$$

$$k_{HD}/k_2^{1/2}=[(CF_3H)_t/(C_2F_6)_t^{1/2}t^{1/2}(HD)_{Av}]-[k_{H_2}(H_2)_{Av}/k_2^{1/2}(HD)_{Av}], \quad (G)$$

$$k_{DH}/k_2^{1/2}=[(CF_3D)_t/(C_2F_6)_t^{1/2}t^{1/2}(HD)_{Av}]-[k_{D_2}(D_2)_{Av}/k_2^{1/2}(HD)_{Av}], \quad (H)$$

$$k_{D_2}/k_2^{1/2}=[(CF_3D)_t/(C_2F_6)_t^{1/2}t^{1/2}(D_2)_{Av}]-[k_{DH}(DH)_{Av}/k_2^{1/2}(D_2)_{Av}]. \quad (I)$$

In most of the runs with D_2, the fluoroform was not analyzed mass spectrometrically. In this case, Eq. (J) was used instead of Eq. (I):

$$k_{D_2}/k_2^{1/2}=\{[(CF_3H)_t+(CF_3D)_t]/(C_2F_6)_t^{1/2}t^{1/2}(D_2)_{Av}\}-[(k_{HD}+k_{DH})(HD)_{Av}/k_2^{1/2}(D_2)_{Av}]. \quad (J)$$

The two equations gave concordant results in cases where they could be compared. The second term in Eqs. (F)–(J) is a correction required by the presence of isotopic impurities in the hydrogen. These terms involve rate constant ratios which are themselves being determined, but they were always small and at a given temperature a self-consistent set of ratios was easily obtained.

Experimental conditions, reactant and product concentrations, and calculated abstraction/recombination rate constant ratios are presented in Tables I–III for runs with H_2, HD, and D_2, respectively. Rate constant ratios k_{H_2}/k_{D_2} for runs with H_2–D_2 mixtures are included in Table III, and the k_{HD}/k_{DH} ratios are included in Table II. The entries for C_3F_8 will be explained below.

Figure 1 presents the data for abstraction from H_2, HD, and D_2, relative to recombination, as a plot of log$r$ (the rate constant ratio) versus $10^3/T$. Figure 2 is the analogous plot for k_{HD}/k_{DH} and k_{H_2}/k_{D_2} obtained from competitive experiments. The data cover the temperature range 365°–605°K. These plots should be linear if the Arrhenius expression is obeyed:

$$\log k=\log A-E_a/2.3RT. \quad (K)$$

It is apparent that, with the exception of the k_{H_2}/k_{D_2} ratio, the plots are not linear over this temperature range. Both the pre-exponential factor and the activation energy derived from Eq. (K) increase with increasing temperature for the ratio r, while the corresponding quantities for the k_{HD}/k_{DH} ratio decrease with increasing temperatures.

Therefore, several attempts were made to fit the data with an expression in which a third term was added to Eq. (K). A least-squares program was used to evaluate the coefficients in this three-term expression, where the

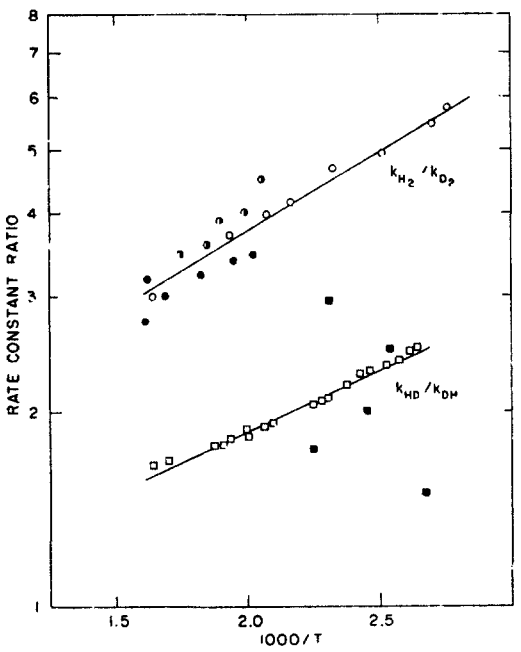

FIG. 2. Experimental isotopic rate constant ratios as a function of temperature. Results obtained from separate measurements with H_2 and D_2 are not included. ○, CF_3+H_2/D_2, this work; ●, same reaction, Ref. 5; ◑, $C_3F_7+H_2/D_2$, Ref. 11; □, CF_3+HD, this work; ■, same reaction, Ref. 6. Solid lines, best least-squares Arrhenius fit with parameters from Table V.

TABLE I. CF_3COCF_3 photolysis with added H_2.

$10^3/T$ (°K)$^{-1}$	$k_{H_2}/k_2^{1/2}$ (liter$^{1/2}$ mole$^{-1/2}$. sec$^{-1/2}\times 10^2$)	Time (sec)	CF_3COCF_3 ($M\times 10^4$)	H_2 ($M\times 10^4$)	C_2F_6 ($M\times 10^6$)	CF_3H ($M\times 10^6$)	C_3F_8 ($M\times 10^6$)
1.655	275	3 600	5.13	6.49	0.361	18.82	0.0044
1.656	285	7 220	1.14	3.12	0.103	7.36	0.0019
1.658	264	3 600	3.56	5.84	0.613	20.84	0.0067
1.659	270	4 860	4.90	4.21	0.415	14.99	0.0055
1.768	166	7 200	4.91	2.30	2.619	13.90	0.0532
1.894	70.7	7 200	5.66	15.08	0.978	27.00	0.0104
1.947	47.7	7 200	5.33	4.00	3.581	9.205	0.0488
2.075	27.8	7 200	3.60	2.47	2.749	3.013	0.0386
2.080	27.2	7 200	4.93	3.34	3.528	17.95	0.0314
2.170	16.8	7 200	8.46	4.17	6.370	4.679	0.0425
2.239	9.36	14 400	6.05	61.77	2.788	36.10	0.1364
2.299	6.56	14 400	7.90	55.53	5.861	33.04	0.1873
2.329	6.65	7 200	9.36	4.65	7.380	2.120	0.0624
2.369	5.75	7 200	5.52	10.15	4.427	3.300	0.0532
2.426	3.62	7 200	6.15	14.71	5.066	3.202	0.0439
2.468	3.36	7 200	5.83	26.14	4.682	5.129	0.0916
2.527	2.44	7 200	4.81	12.37	4.226	1.674	0.0497
2.588	1.66	3 600	5.94	5.94	3.091	0.331	0.0046
2.643	1.46	7 200	6.71	17.31	5.620	1.607	0.0532
2.660	1.22	3 600	1.34	8.01	0.505	0.181	0.0024
2.707	1.05	7 200	5.78	8.68	5.066	0.553	0.0317
2.763	0.769	7 200	6.80	4.54	5.364	0.222	0.0166
3.382	0.039	4 900	0.93	6.43	0.590	0.0043	n.d.[a]
3.388	0.043	7 200	1.95	7.11	0.840	0.0075	n.d.

[a] n.d.—not detected.

TABLE II. CF_3COCF_3 photolysis with added HD.

$10^3/T$ (°K)$^{-1}$	$(k_{HD}+k_{DH})/k_2^{1/2}$ (liter$^{1/2}$ mole$^{-1/2}$. sec$^{-1/2}\times 10^2$)	k_{HD}/k_{DH}	Time (sec)	CF_3COCF_3 ($M\times 10^4$)	HD ($M\times 10^4$)	C_2F_6 ($M\times 10^6$)	C_3F_8 ($M\times 10^6$)	$[CF_3H+CF_3D]$	(CF_3H/CF_3D)
1.652	170.5	1.622	3600	6.55	6.06	0.873	0.0083	17.668	1.653
1.653	186.2	1.647	4800	4.34	6.78	0.535	0.0065	19.988	1.696
1.761	87.85	1.667	7200	3.30	4.03	1.426	0.0370	11.154	1.711
1.870	44.46	n.m.[a]	7200	7.66	8.51	3.394	0.0601	18.420	
1.884	38.10	1.760	7200	7.90	11.21	2.936	0.0509	19.479	1.794
1.922	32.88	1.765	7200	10.06	10.16	4.162	0.0555	18.089	1.802
1.943	31.66	1.818	8640	3.59	5.91	2.721	0.0543	8.999	1.847
2.017	18.59	1.871	7560	7.76	12.18	3.584	0.0539	11.879	1.902
2.028	18.54	1.846	7200	4.37	7.32	2.925	0.0324	6.284	1.885
2.054	16.43	n.m.	7500	7.96	7.57	4.878	0.0144	7.752	
2.078	15.57	1.886	7200	4.01	8.98	2.728	0.0486	6.247	1.924
2.110	11.17	1.919	7200	5.78	20.64	2.467	0.0532	9.893	1.964
2.170	7.732	n.m.	7200	5.90	11.16	4.531	0.0254	5.026	
2.226	5.796	n.m.	7200	5.66	11.10	3.752	0.0416	3.417	
2.229	5.806	n.m.	7560	7.52	6.80	5.197	0.0301	2.527	
2.234	5.698	n.m.	7200	5.42	9.31	3.852	0.0356	2.851	
2.251	4.911	2.027	7200	4.65	11.88	2.504	0.0532	2.536	2.070
2.287	4.007	2.081	7320	7.92	15.89	5.202	0.0243	4.028	2.125
2.308	4.301	2.097	7200	7.32	12.59	3.977	0.0301	2.969	2.133
2.384	2.694	2.170	7200	7.66	17.30	7.109	0.0423	3.415	2.213
2.425	2.358	2.247	7200	5.98	33.56	4.934	0.0849	4.210	2.299
2.464	1.754	2.306	7200	6.43	17.52	6.298	0.0432	2.127	2.351
2.526	1.213	2.345	7200	6.05	56.18	4.753	0.0486	4.117	2.396
2.585	0.985	2.405	7200	5.41	22.65	5.098	0.0439	1.383	2.450
2.644	0.694	2.502	7200	6.45	19.66	5.963	0.0335	0.919	2.550
2.711	0.489	n.m.	7200	10.80	19.14	9.082	0.0284	0.777	(>2.4)
2.763	0.394	n.m.	7320	5.49	15.37	5.142	0.0187	0.399	(>2.5)

[a] n.m.—not measured.

TABLE III. CF_3COCF_3 photolysis with added D_2.

$10^3/T$ (°K)$^{-1}$	$k_{D_2}/k_2^{1/2}$ (liter$^{1/2}$ mole$^{-1/2}$. sec$^{-1/2}\times 10^2$)	k_{H_2}/k_{D_2}	Time (sec)	CF_3COCF_3 ($M\times 10^4$)	D_2 ($M\times 10^4$)	C_2F_6 ($M\times 10^5$)	C_3F_8 ($M\times 10^5$)	CF_3D ($M\times 10^5$)
1.659	89.79	3.005	4 860	4.90	9.45	0.415	0.0055	11.81
1.662	89.60	n.m.	3 600	4.72	6.88	0.953	0.0176	11.29
1.778	43.69	n.m.	7 200	4.03	3.59	3.066	0.0578	7.174
1.904	20.67	n.m.	7 200	7.68	7.16	5.817	0.0694	9.463
1.947	12.89	3.702	7 200	5.33	4.20	3.581	0.0314	2.740
2.075	7.027	3.957	7 200	3.60	6.73	2.749	0.0386	2.111
2.170	4.107	4.090	7 200	8.46	10.96	6.370	0.0425	3.061
2.253	2.351	n.m.	10 860	7.50	12.85	8.816	0.0532	3.019
2.297	1.810	n.m.	7 200	4.38	12.55	4.330	0.0277	1.297
2.299	1.743	n.m.	15 600	6.35	79.81	8.730	0.1572	16.573
2.329	1.440	4.620	7 200	9.36	19.52	7.380	0.0624	1.914
2.369	1.249	4.610	7 200	5.52	15.76	4.427	0.0717	1.122
2.426	0.888	n.m.	7 380	5.96	14.85	6.291	0.0236	0.924
2.468	0.715	4.704	7 200	5.83	16.69	4.682	0.0916	0.701
2.527	0.501	4.873	7 200	4.81	17.13	4.226	0.0497	0.479
2.530	0.497	n.m.	7 235	6.18	24.91	5.892	0.0187	0.833
2.588	0.386	n.m.	7 200	5.83	19.82	5.500	0.0201	0.496
2.622	0.295	n.m.	7 200	10.85	34.72	8.973	0.0125	0.831
2.707	0.194	5.391	7 200	5.78	10.80	5.066	0.0317	0.128
2.763	0.140	5.514	7 200	6.80	16.19	5.364	0.0166	0.142

[a] n.m —not measured.

third term was of the form $\log T$, T, T^{-2}, etc. In these calculations, all data points were given equal weight, the temperature was used as the precise independent variable, and the rate constant ratio was the dependent variable. The effect of the various third terms was determined from the goodness-of-fit, defined by

$$\mathrm{GOF}=\sum_i (m_i-c_i)^2/(k-j).$$

In this expression, m_i is the measured value of the dependent variable at temperature T_i, c_i is the corresponding value calculated from the best-fit equation, k is the number of experimental points, and j is the number of parameters.

The addition of a third term improved the goodness-of-fit by about 50%, but no three-parameter equation was found which was superior to the others, and the errors in the fitted coefficients were considerably larger when an extra term was added. Since no equation was clearly superior, we have chosen to present the one which is the simple expansion of $\log r$ in terms of $(10^3/2.3RT)$:

$$\log r=A+B(10^3/2.3RT)+C(10^3/2.3RT)^2. \quad \text{(L)}$$

Table IV presents the coefficients for the best fit of Eq. (L), as well as the goodness of fit. Addition of a fourth term did not yield much improvement in the goodness of fit, and gave further increases in the errors of the coefficients, so this approach was not pursued. Since the over-all Arrhenius fit is not much worse, the coefficients and goodness-of-fit for

$$\log r=A+B(10^3/2.3RT) \quad \text{(M)}$$

are presented in Table V. For this equation the points calculated using the best-fit coefficients deviate from the experimental points in a systematic manner, lying below the experimental points at the extremes of the temperature range and above them in the middle of the temperature range. Therefore the Arrhenius equation is a poor representation of the data over the entire temperature range and the frequency factors and activation energies obtained from it must be viewed accordingly as rough averages.

IV. COMPARISON WITH OTHER EXPERIMENTAL WORK ON THIS AND RELATED REACTIONS

Several comparisons can be made between our work and that of others on this same reaction or related reactions. Values of the rate constant ratio r (abstraction/recombination) for H_2, D_2, and HD were determined by Ayscough and Polanyi[6] in a system analogous to ours. Their results, shown in Fig. 1, agree well with those we have obtained, although there are systematic trends which will lead to differences in activation energy between the two sets of data.

Pritchard *et al.*[5] did not measure r, but did obtain the isotopic ratio k_{H_2}/k_{D_2} using mixtures of H_2 and D_2. The fact that CF_3 radicals were generated in their experiments by the decomposition of $CF_3N_2CF_3$ instead of by photolysis of hexafluoroacetone should not be significant, and their rate constant ratios are in good agreement with ours (Fig. 2). Ayscough and Polanyi measured k_{HD}/k_{DH}, but their experiment was complicated by the use of an equilibrium mixture of H_2, HD, and D_2. Consequently, substantial corrections for reaction with H_2 and D_2 are necessary, and a large scatter in values of k_{HD}/k_{DH} is found. They did not determine k_{H_2}/k_{D_2} by a competitive method, and values obtained from their individual rate constant measurements are considerably higher than ours.

TABLE IV. Three-parameter least-squares fit to data.

Ratio[a]	A[b]	B[c]	C[d]	Goodness of fit[e]
$k_{H_2}/2k_2^{1/2}$	4.96±0.36	−14.94±1.61	4.46±1.64	0.0015
$k_{HD}/k_2^{1/2}$	5.35±0.41	−17.23±1.77	7.00±1.91	0.0011
$k_{DH}/k_2^{1/2}$	5.09±0.39	−16.55±1.69	5.36±1.82	0.0010
$k_{D_2}/2k_2^{1/2}$	4.59±0.26	−14.92±1.07	3.46±1.09	0.00058
$k_{H_2}{}^f/k_{D_2}$	−0.048±0.117	1.71±0.50	−0.64±0.54	0.000066
$k_{HD}{}^f/k_{DH}$	0.182±0.043	−0.40±0.20	1.36±0.18	0.00013

[a] $\log_{10}(\text{ratio}) = A + B(10^3/2.3RT) + C(10^3/2.3RT)^2$. Ratio in units of (liter per mole·second)$^{1/2}$ for abstraction/recombination, dimensionless for isotope effects.
[b] A in same units as $\log_{10}$(ratio).
[c] B in units of kcalories per mole.
[d] C in units of (kcalories per mole)^2.
[e] Goodness of fit as defined in text. Here $j=3$.
[f] These are from data of competitive experiments and are not derived from the separate abstraction/recombination ratios.

If the three-center approximation to the transition state (discussed below) is valid, other alkyl radicals reacting with hydrogen isotopes should produce isotope effects very similar to those we have observed. This is indeed the case for C_3F_7 radicals produced by the photolysis of perfluorodi-*n*-propyl ketone[11] in the presence of H_2–D_2 mixtures. The same reaction was studied by Pritchard and Foote,[12] who photolyzed the corresponding perfluoropropyl aldehyde. However, they did not use mixtures of H_2 and D_2 and the isotopic rate constant ratios obtained by them are generally higher than those of Miller and Steacie.[11] Their analogous experiments with C_2F_5 radicals give values of k_{H_2}/k_{D_2} which are also high, and which have an abnormally small temperature dependence. The closest approximation to the CF_3 reaction is probably found in the work of Hautecloque,[13] who studied the photolysis of CCl_3Br and the subsequent reactions of CCl_3 with H_2 and D_2. Again, unfortunately, these experiments did not make use of the isotopic competition method; nevertheless, the rate constant ratios are in close agreement with ours. Majury and Steacie[14] and Whittle and Steacie[15] have measured rate constants for reactions of CH_3 and CD_3 with H_2, HD, and D_2. Here again, competitive rate constant measurements were not made, and it does not seem useful to make a detailed comparison of experimental results, although there is rough agreement between the magnitudes of analogous isotope effects in the methyl and trifluoromethyl systems.

TABLE V. Least-squares fit of data to the Arrhenius equation.

Ratio[a]	A[b]	B[c]	Goodness of fit[d]
$k_{H_2}/2k_2^{1/2}$	3.97±0.065	−10.66±0.14	0.0022
$k_{HD}/k_2^{1/2}$	3.87±0.069	−10.77±0.15	0.0017
$k_{DH}/k_2^{1/2}$	3.98±0.061	−11.63±0.13	0.0014
$k_{D_2}/2k_2^{1/2}$	3.84±0.056	−11.66±0.11	0.0012
k_{H_2}/k_{D_2}	0.113±0.022	1.05±0.05	0.00011
k_{HD}/k_{DH}	−0.109±0.013	0.86±0.02	0.000043

[a] $\log_{10}(\text{ratio}) = A + B(10^3/2.3RT)$. Ratio units as for Table IV.
[b] A in same units as $\log_{10}$(ratio).
[c] B in units of kcalories per mole.
[d] Goodness of fit as defined in text. Here $j=2$.

V. TEMPERATURE DEPENDENCE OF RATE CONSTANT RATIOS

The curvature observed in the plots of log$r$ against T^{-1} could be attributed to a pressure dependence of the radical reactions, to hot radical reactions, to quantum mechanical tunneling, or simply to the oversimplification of the temperature dependence which is given by an Arrhenius equation.

Arthur and Bell[16] have found the recombination rate for CF_3 radicals to be third order at temperatures above 500°C in the thermal decomposition of CF_3CHO. This would result from the formation of an excited C_2F_6 molecule which can either dissociate or be stabilized by collision, according to

$$2CF_3 \xrightarrow{k_2} C_2F_6^*, \tag{7}$$

$$C_2F_6^* \xrightarrow{k_d} 2CF_3, \tag{8}$$

$$M + C_2F_6^* \xrightarrow{k_s} C_2F_6 + M. \tag{9}$$

Then,

$$\frac{d(C_2F_6)}{dt} = \frac{k_2 k_s M(CF_3)^2}{k_s M + k_d}$$

and

$$\frac{k_{H_2}{}^2}{k_2}\left(1+\frac{k_d}{k_s M}\right) = \frac{k_{H_2}{}^2}{k_r} = \frac{[\text{rate}(CF_3H)]^2}{[\text{rate}(C_2F_6)](H_2)^2}. \tag{N}$$

Thus, $k_{H_2}/k_r^{1/2}$ and not $k_{H_2}/k_2^{1/2}$ is measured. Higher temperatures (larger k_d) or lower pressures (smaller $k_s M$) would cause $k_{H_2}{}^2/k_r$ to be greater than $k_{H_2}{}^2/k_2$, if the recombination is in the third-order region. To test

[11] G. H. Miller and E. W. R. Steacie, J. Am. Chem. Soc. **80**, 6486 (1958).
[12] G. O. Pritchard and J. K. Foote, J. Phys. Chem. **68**, 1016 (1964).
[13] S. Hautecloque, Compt. Rend. **261**, 3613 (1965).
[14] T. G. Majury and E. W. R. Steacie, Discussions Faraday Soc. **14**, 45 (1953).
[15] E. Whittle, Discussions Faraday Soc. **14**, 120 (1953); E. Whittle and E. W. R. Steacie, J. Chem. Phys. **21**, 993 (1953).
[16] N. L. Arthur and T. N. Bell, Chem. Comm. **1965**, 166.

TABLE VI. Pressure dependence of abstraction/recombination rate ratio.

T (°K)	$(CF_3COCF_3)^{-1}$[a]	$k_{H_2}^2/k_r$[b]	k_0[c]
376	7.4	1.58	1.29
376	17.0	1.63	1.28
376	24.0	1.56	1.26
376	37.5	1.78	1.05
604	8.7	8500	5.5
604	18.3	9030	4.0
604	32.3	9680	3.1

[a] Units of liter per mole $\times 10^3$. $(H_2)/(CF_3COCF_3) \approx 5$.
[b] Units of liter mole^{-1}·sec$^{-1} \times 10^{-3}$.
[c] $d(CF_3COCF_3)/dt = k_0(CF_3COCF_3)$; k_0 in units of (second^{-1}).

Eq. (N) at 376° and 604°K, $k_{H_2}^2/k_r$ was determined as a function of total pressure. The results are given in Table VI and Fig. 3. At the lower temperature, the effect of pressure on $k_{H_2}^2/k_r$ is very slight, but the higher temperature runs show a noticeable increase of this quantity with increasing values of $1/(CF_3COCF_3)$. As predicted by Eq. (N), the dependence is linear. Therefore, the recombination does become third order at lower pressures. The infinite pressure intercept gives $k_{H_2}^2/k_r = k_{H_2}^2/k_2$; the shaded area of Fig. 3 indicates the pressure range covered in the isotope effect experiments, and it is evident that even at the higher temperature, these quantities are nearly identical. Hence, for our purposes, the recombination reaction may be considered second order, and the curvature of the Arrhenius plots is not due to a change in the order of this reaction.

Also included in Table VI are values for the first-order decomposition rate of CF_3COCF_3. These seem to decrease at very low pressures, not significantly for the low-temperature runs, but quite rapidly at the high temperatures where the quantum yield is apparently greater than unity.

It seems unlikely that hot radical reactions are responsible for the nonlinear temperature dependence. The abstraction rates were essentially the same whether or not the illumination contained 2537-Å radiation; this was true even at lower temperatures where hot reactions would be most conspicuous. Quenching effects at high pressures were also absent.

The problem of quantum-mechanical tunneling is discussed in some detail below. It is sufficient to say at this point that the amount of tunneling predicted by the transition state models used to describe the isotope effects would produce curvature of magnitude similar to that observed experimentally. It is also likely that, apart from tunneling, the simple Arrhenius expression does not adequately express the temperature dependence of a rate constant over a very wide temperature range. Hence, the activation energy derived from this expression is an approximation to the actual energy difference between reactants and transition state.

VI. STEADY-STATE HYDROGEN ATOM CONCENTRATION

It was important in this work to determine the fate of the hydrogen and deuterium atoms formed in the CF_3 abstraction reactions, since the occurrence of Reactions (10) and (11) would produce errors in the observed isotope effects:

$$CF_3 + H \xrightarrow{k_H} CF_3H, \quad (10)$$

$$CF_3 + D \xrightarrow{k_D} CF_3D. \quad (11)$$

In their study of the reactions of CF_3 and the hydrogen isotopes, Ayscough and Polanyi[6] disregarded these reactions on the basis of kinetic arguments. On the other hand, Price and Kutschke,[17] investigating the reactions of C_2F_5 with H_2, assumed that *all* hydrogen atoms disappeared by radical–atom recombination. The ambiguity of these results has been further discussed by Kutschke.[18]

From our data, the stationary-state CF_3 concentration was estimated from observed rates of formation of C_2F_6 and Ayscough's value[19] for the recombination rate constant. Upper limits on the hydrogen and deuterium atom concentrations were obtained from the observed rates of isotopic scrambling (H_2 and D_2 from HD, and vice versa) together with LeRoy's values[20] for the various hydrogen atom–hydrogen molecule reaction rates. The estimated radical and atom concentrations thus obtained are shown in Table VII. The second-order recombination rate for hydrogen atoms in the gas phase can be estimated to be about 5×10^7 liter mole^{-1}·sec^{-1} in these experiments. This value is derived from the corresponding third-order rate

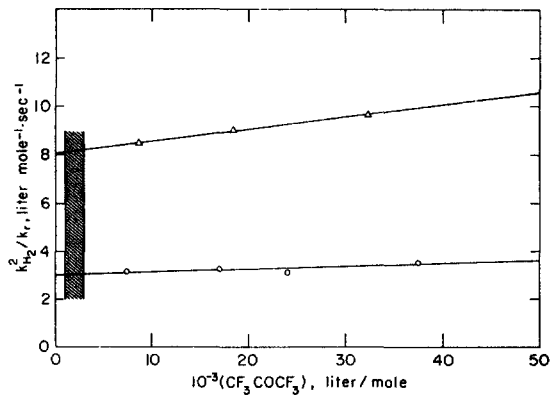

FIG. 3. Pressure dependence of $k_{H_2}^2/k_r$. The shaded area indicates the pressure region used in the isotope effect experiments. Circles, 376°K; triangles, 604°K.

[17] S. J. W. Price and K. O. Kutschke, Can. J. Chem. **38**, 2128 (1960).
[18] K. O. Kutschke, Can. J. Chem. **42**, 1232 (1964).
[19] P. B. Ayscough, J. Chem. Phys. **24**, 944 (1956).
[20] D. J. Le Roy, B. A. Ridley, and K. A. Quickert, Discussions Faraday Soc. **44**, 92 (1968); earlier references cited therein.

TABLE VII. Estimated steady-state atom and radical concentrations and radical–atom recombination rates.

T(°K)	Added gas	(CF_3)	(H)	(D)	CF_2H[a]	CF_3H[b]	CF_3D[a]	CF_3D[b]
		$10^{12}\times$conc (M)			$10^{12}\times$rate of formation (M sec^{-1})			
433	HD	500	0.4	0.6	2 800	0.2	1 300	0.3
433	H_2, D_2	660	1.1	1.1	2 940	0.7	2 660	0.7
514	H_2, D_2	465	2.1	0.7	1 300	1.0	3 800	0.3
605	HD	220	2.2	3.9	26 000	0.5	15 000	0.9

[a] Total rate of formation (abstraction+recombination). [b] Rate of formation from radical–atom recombination.

constant obtained in hydrogen[21] and the assumption that the third-body efficiency of the reaction mixture in our experiments is the same as that of hydrogen. The rate constant for CF_3 recombination[19] is 2×10^{10} liter mole^{-1}·sec^{-1}, and one would expect rate constants for Reactions (10) and (11) to lie somewhere between this and the value for H-atom recombination. With a value of 10^9 liter mole^{-1}·sec^{-1} for k_H and k_D, rates of formation of CF_3H and CF_3D from Reactions (10) and (11) are estimated and compared in Table VII with total rates of formation of these products. Atom–radical reaction rates are seen to be completely negligible; they are less than 1% of the total rates even if k_H and k_D are comparable to the CF_3 recombination rate constant. This depends on the extremely low stationary-state concentration of atoms, which must be due to rapid recombination on the surface. Since much of the exchange of hydrogen isotopes must occur this way also, the actual homogeneous exchange rate must be lower than estimated. Therefore, the atom concentrations and the radical–atom reaction rates are probably lower than those given in Table VII.

It is more difficult to rule out atom–radical recombination on the surface, especially since the atom–atom recombination there is so efficient. However, runs with hexafluoroacetone alone, following a run with added hydrogen, gave yields of fluoroform approximately 0.1% of the analogous yield in the presence of hydrogen, so that scavenging of hydrogen atoms from the surface is not very efficient. The errors this would produce in the isotope effect measurements would be of the same magnitude, and less than the accumulated errors from other sources.

Two runs at 396°K, one with D_2 added and the other with an approximately equivalent pressure of a 3:4 H_2–D_2 mixture, gave identical values of $k_{D_2}/k_2^{1/2}$. In the latter case, the fraction of atoms formed which are deuterium atoms was about 0.2. Both the surface coverage and the rate of recombination of CF_3 and D on the surface should be decreased by approximately this factor compared to the run with D_2 alone. Since no difference in $k_{D_2}/k_2^{1/2}$ was detected, radical–atom recombination on the surface must be negligible compared to the abstraction reaction.

We conclude that homogeneous radical–atom, atom–atom, and exchange reactions are not important in our reaction systems, due to the low stationary-state concentration of hydrogen atoms. At the surface, hydrogen atom recombination is very rapid, but radical–atom recombination is unimportant compared to the abstraction reactions studied.

VII. YIELDS OF MINOR PRODUCTS

Photolysis of hexafluoroacetone in the presence of hydrogen gave C_3F_8 and C_2F_5H in addition to the expected products CO, C_2F_6, and CF_3H. These additional products formed 0.1%–1% of the total in most runs, their yield increasing with longer photolysis times and increasing slightly with increasing temperature. The yields were also noticeably greater with hydrogen present than in runs with hexafluoroacetone alone (cf. Tables I–III).

The ratio $(C_2F_5H)/(C_3F_8)$ varies in much the same manner as the ratio $(CF_3H)/(C_2F_6)$, indicating that C_2F_5H and C_3F_8 are probably formed by reactions of C_2F_5 radicals such as

$$C_2F_5+CF_3\xrightarrow{k_2'}C_3F_8, \tag{12}$$

$$C_2F_5+H_2\xrightarrow{k_{H_2}'}C_2F_5H+H. \tag{13}$$

We are unable to account for the presence of these radicals. They may be formed directly or by th reaction

$$CF_3+CF_2\rightarrow C_2F_5. \tag{14}$$

Trenwith and Batey[22] found that CF_2 was produced in the thermal decomposition of hexafluoroacetone at 600°C, according to

$$CF_3COCF_3\rightarrow CF_3COF+CF_2. \tag{15}$$

In addition, $CH_3CF_2CH_3$ has been found in the photolysis of trifluoroacetone, and Kutschke has previously reported finding C_3F_8 in studies of hexafluoroacetone photolysis.[23] Since tetrafluoromethane has never been observed in our work or that of others on the photolysis of hexafluoroacetone, it seems unlikely that CF_2 results from the disproportionation of CF_3 radicals. Recom-

[21] F. S. Larkin and B. A. Thrush, Discussions Faraday Soc. **37**, 112 (1964).

[22] W. Trenwith and A. B. Batey, J. Chem. Soc. **1961**, 1388.

[23] K. O. Kutschke (private communication).

TABLE VIII. Relative amounts of CF_3 and C_2F_5 products in photolyses with added HD.

$10^3/T$ (°K^{-1})	$(C_2F_6)^a$	(C_3F_8)	$(CF_3H)+(CF_3D)$	$(C_2F_5H)+(C_2F_5D)$	R^b
1.652	0.873	0.0083	17.67	0.0437	0.26
1.653	0.535	0.0065	19.99	0.0374	0.16
1.761	1.426	0.0370	11.15	0.0509	0.18
1.870	3.394	0.0601	18.42	0.0546	0.17
1.884	2.936	0.0509	19.48	0.0486	0.14
1.922	4.162	0.0555	18.09	0.0416	0.17
1.943	2.721	0.0543	9.00	0.0410	0.23
2.017	3.584	0.0539	11.88	0.0393	0.22
2.028	2.925	0.0324	6.28	0.0208	0.30
2.054	4.878	0.0144	7.75	0.0062	0.27
2.078	2.728	0.0486	16.25	0.0185	0.17
2.170	4.531	0.0254	5.03	0.0076	0.27
2.229	5.197	0.0301	2.53	0.0030	0.20
2.287	5.202	0.0243	4.03	0.0065	0.34
2.425	4.934	0.0849	4.21	0.0150	0.21
2.526	4.753	0.0486	4.12	0.0083	0.20

[a] All concentrations in units of $M\times10^{-5}$.
[b] $R=[(C_2F_5H)+(C_2F_5D)](C_2F_6)/[(CF_3H)+(CF_3D)](C_3F_8)$.

bination of CF_2 radicals should yield C_2F_4, while the recombination of C_2F_5 radicals should yield C_4F_{10}. Neither of these products was formed in quantities sufficient for detection, due to the very low radical concentrations.

Relative yields of the products apparently resulting from C_2F_5 reactions and those from CF_3 reactions can be related to the appropriate rate constants; this was done in detail only for the case of HD. The appropriate expression is

$$R=\left(\frac{k_a'}{k_a}\right)\left(\frac{k_2}{k_2'}\right)$$

$$=\frac{(C_2F_5H)_t+(C_2H_5D)_t}{(CF_3H)_t+(CF_3D)_t}\frac{(C_2F_6)_t}{(C_3F_8)_t}, \qquad (O)$$

where k_a is the sum of k_{HD} and k_{DH} and k_a' is the analogous expression for C_2F_5 reactions. The data given in Table VIII indicate that R is temperature independent, and since one would expect k_2/k_2' to be almost unaffected by temperature changes, the implication is that the activation energy for abstraction by C_2F_5 is equal to that for CF_3 radicals. Previously reported values[12,17] for the reaction of C_2F_5 with H_2 are 11.9 and 12.4 kcal/mole, compared with our value of 10.7 for CF_3 with H_2. However, the difference of ~1 kcal/mole is probably too small to be detected in our experiments, where the C_2F_5 radical concentration is very low.

It seems unlikely that CF_2 and C_2F_5 are primary products of the decomposition of hexafluoroacetone, since their yields increase with longer photolysis times. Addition of CF_3 radicals or H atoms to hexafluoroacetone and subsequent photolysis of the addition product may be involved in the formation of these minor products. The presence of the OH group was indicated by a band at 3650 cm^{-1} in the infrared spectrum of the hexafluoroacetone fraction which remained after a run. Hexafluoroacetone hydrate also has an absorption band in this region. Gordon[24] reported the formation of $(CF_3)_3COCF_3$ during the photolysis of hexafluoroacetone; hence, in the presence of hydrogen, one would anticipate the possible production of $(CF_3)_3COH$ and $(CF_3)_2HCOCF_3$. Material balance estimates indicate that about one-third of the hydrogen consumed forms products other than fluoroform, but the small extent of reaction made it impossible to determine this precisely. No serious attempt was made to isolate, identify, and measure the yield of possible addition products.

Fortunately, none of the minor side reactions appears to affect either the abstraction/recombination rate constant ratios or the isotopic rate constant ratios. This is probably because the very low extent of reaction prevented appreciable buildup of minor by-products.

VIII. VIBRATIONAL FORCE FIELDS AND FREQUENCIES

The geometry and internal coordinates assumed for the complete six-atom activated complex are shown in Fig. 4. The linear configuration of the H–H–C group is based on the general prediction of semiempirical methods for three-atom transition states in hydrogen abstraction reactions. Neither the further assumption of C_{3v} symmetry nor the dimensions used for the CF_3 group have an important effect on the calculations of vibrational frequencies. The most general form of the

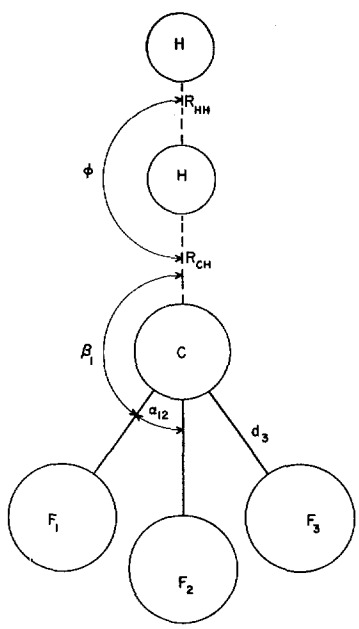

FIG. 4. Assumed geometry of the activated complex for CF_3+H_2.

[24] A. S. Gordon, J. Chem. Phys. **36**, 1330 (1962).

TABLE IX. Force constant sets and corresponding vibrational frequencies for CF_3 and H–H–CF_3.

Force constant	Force constant set								
	I	TS-I	II	TS-IIa	TS-IIb	TS-IIc	TS-IIIa	TS-IIIb	TS-O
F_{CH}[a]	···	0.883	···	0.883	0.883	0.883	0.565	0.598	0.883
F_{HH}[a]	···	1.495	···	1.495	1.495	1.495	0.689	0.728	1.495
F_{int}[a]	···	1.898	···	1.898	1.898	1.898	1.704	1.689	1.898
F_ϕ[b]	···	0.0521	···	0.0521	0.0521	0.0521	0.0838	0.0835	0.0521
F_β[b]	···	0.41	···	0.001	0.41	0.80	0.41	0.41	···
F_d[a]	5.60	5.60	6.35	6.35	6.35	6.35	6.35	6.35	···
F_{dd}[a]	0	0	0.65	0.65	0.65	0.65	0.65	0.65	···
F_α[b]	1.26	1.26	1.78	1.78	1.78	1.78	1.78	1.78	···
$F_{\alpha\alpha}$[b]	0	0	0.50	0.50	0.50	0.50	0.50	0.50	···
$F_{d\alpha}$[c]	0	0	0.50	0.50	0.50	0.50	0.50	0.50	···
$F_{d\alpha}'$[c]	0	0	−0.50	−0.50	−0.50	−0.50	−0.50	−0.50	···
Vibration	Frequencies in cm^{-1}								
$\nu_1(a_1)$		**1720**		**1732**	**1738**	**1742**	**1468**	**1475**	**1703**
$\nu_2(a_1)$	943	925	1112	1048	1071	1094	1036	1038	
$\nu_3(a_1)$	452	495	664	652	682	706	680	681	
$\nu_4(a_1)$		**1613i**		**1610i**	**1610i**	**1609i**	**2072i**	**2019i**	**1626i**
$\nu_5(e)$	1329	1379	1170	1172	1240	1413	1258	1258	
$\nu_6(e)$		**972**		**650**	**954**	**1064**	**1019**	**1018**	**654**
$\nu_7(e)$	464	464	499	498	498	498	499	499	
$\nu_8(e)$		**286**		**22**	**285**	**313**	**315**	**315**	

[a] In units of millidynes per angstrom. [b] In units of millidyne-angstroms. [c] In units of millidynes.

vibrational potential energy function which was used is

$$2V = F_{CH}(\Delta R_{CH})^2 + F_{HH}(\Delta R_{HH})^2 + F_{int}(\Delta R_{CH})(\Delta R_{HH})$$
$$+ 2F_\phi(\Delta\phi)^2 + F_{dd}[(\Delta d_1)^2 + (\Delta d_2)^2 + (\Delta d_3)^2]$$
$$+ 2F_{dd}[(\Delta d_1)(\Delta d_2 + \Delta d_3) + (\Delta d_2)(\Delta d_3)]$$
$$+ F_\alpha[(\Delta\alpha_{12})^2 + (\Delta\alpha_{13})^2 + (\Delta\alpha_{23})^2]$$
$$+ F_\beta[(\Delta\beta_1)^2 + (\Delta\beta_2)^2 + (\Delta\beta_3)^2]$$
$$+ 2F_{\alpha\alpha}[(\Delta\alpha_{12})(\Delta\alpha_{23} + \Delta\alpha_{13}) + (\Delta\alpha_{23})(\Delta\alpha_{13})]$$
$$+ 2F_{d\alpha}[(\Delta d_1)(\Delta\alpha_{12} + \Delta\alpha_{13})$$
$$+ \Delta d_2(\Delta\alpha_{12} + \Delta\alpha_{23}) + \Delta d_3(\Delta\alpha_{23} + \Delta\alpha_{13})]$$
$$+ 2F_{d\alpha}'[(\Delta d_1)(\Delta\alpha_{23}) + (\Delta d_2)(\Delta\alpha_{13}) + (\Delta d_3)(\Delta\alpha_{12})].$$

Two sets of force constants for the CF_3 part of the activated complex were used. Set I (Table IX) corresponds to that used by Sharp and Johnston[3] for the activated complex of the CF_3+CH_4 reaction, with no interaction force constants included. This set did not reproduce the observed frequencies of CF_3H very well. The slightly larger Set II was obtained by iterative least-squares adjustment of the force constants tabulated, with all others constrained to zero. In particular, no interaction terms involving "reaction center" coordinates and "stable molecule" coordinates were included. This procedure led to a set of force constants which gave an average deviation of 4% between calculated and observed frequencies of CF_3H and CF_3D. Force constants for the activated complex were obtained by combining Sets I or II of CF_3 with additional force constants for the degrees of freedom at the reaction center. The latter were obtained from the bond-energy–bond-order (BEBO) treatment (Sets TS-I and TS-II) or from the London–Eyring–Polanyi–Sato (LEPS) method (Set TS-III). In addition, a simple three-atom transition state was considered, with force constants obtained from the BEBO method (Set TS-O).

TABLE X. Properties of reactant and product bonds.

	H–H	C–H
R_e (Å)	0.742	1.09
D_0^0 (kcal/mole)	103.2	106.3
ω (cm^{-1})	4395	3031
D_e[a] (kcal/mole)	109.44	110.60
β ($Å^{-1}$)	1.94	1.78
F (mdyn/Å)	5.74	5.00
p	1.041	1.087

[a] Dissociation energy from minimum of potential curve.

The BEBO, or bond energy–bond order, method derived by Johnston and Parr[25] enables one to calculate the necessary transition state properties of a three-atom system without the introduction of adjustable parameters. The properties of the reactant and product required for its use in the present case are given in Table X. The value of the C–H bond dissociation energy in fluoroform has been the subject of some controversy recently; we have used the value of 106.3±0.5 kcal/mole suggested by Coomber and Whittle.[26] To this is added the zero-point energy of 4.3 kcal/mole corresponding to an observed[27] C–H stretching frequency of 3031 cm^{-1}. The value of the Morse parameter β for the C–H bond

[25] H. S. Johnston and C. Parr, J. Am. Chem. Soc. **85**, 2544 (1963).
[26] J. W. Coomber and E. Whittle, Trans. Faraday Soc. **62**, 2183 (1966).
[27] S. R. Polo and M. K. Wilson, J. Chem. Phys. **21**, 1129 (1953).

TABLE XI. Activation energies.

	BEBO three-atom	BEBO six-atom				LEPS	
		TS-I	TS-IIa	TS-IIb	TS-IIc	TS-IIIa	TS-IIIb
V_a (kcal/mole)	12.56	12.56	12.56	12.56	12.56	13.80	12.88
$\Sigma\theta^\ddagger$	2.05	5.88	4.96	5.86	6.61	5.67	5.68
$\Sigma\theta_r$	5.28	8.25	8.24	8.24	8.24	8.24	8.24
θ^*	−1.87	−1.82	−1.82	−1.82	−1.82	−2.97	−1.88[a]
$(d^\ddagger-d_r)/2$	1.50	2.50	2.50	2.50	2.50	2.50	2.50
ΘRT (kcal/mole)	−3.58	−1.68	−2.58	−1.69	−0.94	−3.01	−1.93
E_a (kcal/mole)[b]	8.98	10.88	9.98	10.87	11.62	10.79	10.95

[a] Johnston–Rapp "averaged" tunneling.

[b] Experimental value at 500°K, 11.04 kcal/mole.

is taken to be equal to that of the same bond in methane, although this is a few percent lower than the value used by Carmichael and Johnston.[28]

The LEPS method includes an adjustable parameter κ which is usually chosen to give agreement between experimental and calculated values of the activation energy, a procedure which we have also followed.

The equations needed for calculation of the vibrational frequencies for a three-atom model have been given elsewhere[29]; for the larger model, modifications of the Schachtschneider programs[30] were used to evaluate the necessary **G** matrices and to solve the vibrational secular equations.

IX. CALCULATION OF ACTIVATION ENERGIES

Experimentally, the activation energy is defined by the expression

$$E_a=-Rd\ \ln k/d(T^{-1}).$$

Transition-state theory gives a rate constant of the form

$$k=B(T)\ \exp(-V_a/RT),$$

where V_a is the actual barrier height of the potential energy surface, or the "potential energy of activation". If a function Θ is defined, such that

$$\Theta=d\ \ln B/d\ \ln T,$$

then

$$E_a=V_a+\Theta RT.$$

For each vibrational degree of freedom,

$$\theta_i=(u_i/2)\ \coth(u_i/2)-1,$$

where

$$u_i=hc\omega_i/kT;$$

while for each translational or rotational degree of freedom (taken to be classical at these temperatures)

$$\theta_{T,R}=-1/2.$$

There is also a contribution from the temperature dependence of the tunneling correction,

$$\theta^*=d\ \ln\Gamma^*/d\ \ln T.$$

This must be evaluated according to the type of correction used, and in our calculations this was simply done numerically. Finally,

$$\Theta=\theta^*+\tfrac{1}{2}(d^\ddagger-d_r)+\sum_{i=1}^{d^\ddagger-1}\theta_i^\ddagger-\sum_{i=1}^{d_r}\theta_i^r,$$

where d is the number of internal degrees of freedom. Since θ_i for vibrations is somewhat temperature dependent, the predicted value of E_a will also be a function of temperature. We have taken 500°K as an average value at which to calculate E_a. The experimental value, evaluated at this same temperature from the three-term expression for $k_{H_2}/2k_2^{1/2}$ in powers of T^{-1}, was 11.04 kcal/mole if there is no activation energy for radical recombination.

The terms contributing to the activation energy are tabulated for various force field assumptions in Table XI. One notes a difference of 1 kcal/mole in E_a between the three-atom and the six-atom models, even when F_β is almost zero; this results from the term $(d^\ddagger-d_r)/2$. For the six-atom model, E_a is a function of F_β, since the bending vibration makes a contribution with a lower limit of zero when $u/2$ is zero. The statement by Carmichael and Johnston[28] that the activation energy is not sensitive to the choice of the three-atom model in place of a more complex transition state is evidently not strictly correct.

We have not calculated the corresponding Arrhenius pre-exponential factors for the various models used, but Sharp and Johnston[3] have already shown that these A factors are influenced strongly by the size of the transition-state model.

X. CALCULATION OF ISOTOPE EFFECTS

Ratios of rate constants k_{H_2}/k_{D_2} and k_{HD}/k_{DH} were calculated in the conventional way[31] from the expression

$$k_1/k_2=(\nu_1^*/\nu_2^*)\,(f_M/f^\ddagger)\,(\tau_1/\tau_2),$$

[28] H. Carmichael and H. S. Johnston, J. Chem. Phys. **41**, 1975 (1964).

[29] R. B. Timmons and R. E. Weston, Jr., J. Chem. Phys. **41**, 1654 (1964).

[30] J. H. Schachtschneider and R. G. Snyder, Spectrochim. Acta **19**, 117 (1963). We are indebted to Dr. Max Wolfsberg for making available to us his modifications of these programs.

[31] J. Bigeleisen and M. Wolfsberg, Advan. Chem. Phys. **1**, 15 (1958).

where ν^* is the imaginary vibrational frequency of the activated complex, and τ is a tunneling correction described below. The quantity f_M is unity for the HD/DH ratio, while for H_2/D_2 it is given by

$$f_{D_2}=(m_D/m_H)^{1/2}\exp[(Z_{H_2}-Z_{D_2})/T],$$

where m is the atomic mass and Z is the sum of vibrational zero-point energy and a rotational correction. The data used were those collected by Persky and Klein,[1] in which case the zero-point energy difference is 889.4°K. However, Wolfsberg[32] has shown recently that the usual way of correcting this energy difference for anharmonicity is not correct; from the spectroscopic data of Herzberg he obtains a zero-point energy difference of 895.2°K. At 333°K, f_{D_2} calculated with this revised value will be larger by 2% than that calculated from the Klein–Persky data. Alternatively, one might neglect anharmonicity corrections for the hydrogen molecule altogether, since they are neglected for the activated complex; this would increase f_{D_2} by 6.6% at 333°K.

The quantity f is the reduced partition function for the activated complex:

$$f^{\ddagger}=\prod_{i=1}^{d^{\ddagger}-1}\frac{u_{2i}^{\ddagger}}{u_{1i}^{\ddagger}}\frac{\sinh(\frac{1}{2}u_{1i}^{\ddagger})}{\sinh(\frac{1}{2}u_{2i}^{\ddagger})},$$

where $d^{\ddagger}-1$ is 4 in the case of a three-atom model and 11 for the complete six-atom model.

Tunneling corrections in all cases were based on the assumption that the potential-energy barrier could be represented by an unsymmetrical Eckart[33] barrier, with parameters of curvature and barrier height chosen as described below. The actual expression for τ is a complicated function of these parameters and the temperature; however, it is easily evaluated numerically with a suitable computer program.

XI. DISCUSSION OF THE BEBO MODEL

Rate constant ratios predicted from this three-atom model are compared with experimental data in Fig. 5. The general agreement is very good, although the predicted temperature dependence of the intramolecular isotope effect is clearly too low.

The BEBO approach does not provide a potential-energy surface, but only a path along which the energy varies. Any tunneling correction is, perforce, for penetration through this one-dimensional barrier. Calculations were made for an Eckart barrier with curvature fitted to that of the actual potential-energy curve at the maximum. The two barrier heights needed are given by the potential energy of activation less the zero-point energy of the reactant hydrogen molecule or the zero-point energy of the product C–H or C–D bond. These tunneling corrections become fairly large at

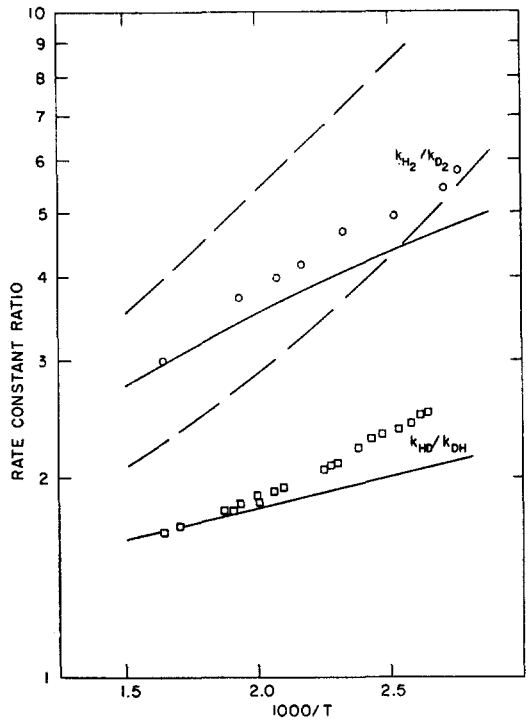

FIG. 5. Isotope effects predicted on the basis of a three-atom BEBO model (force constant set TS-O). —, without tunneling correction; — —, including one-dimensional tunneling correction. Individual points are experimental values.

333°K, and it is likely that they are overestimates. Hence, the fact that their inclusion leads to predicted isotope effects considerably larger than the experimental values (Fig. 5) is not surprising. Qualitatively, one would expect the observed isotope effects to lie somewhere between those predicted in the absence of tunneling and those predicted with an over-simplified model for tunneling.

We next extend the BEBO method to the full six-atom model, with the traditional pious hope that parts of the molecule not actually at the reaction center will not influence the properties of bonds at the reaction center. There is a concommitant assumption that the converse is true, and that force constants for these distant parts of the transition state can be taken from stable molecules. At present, the basis for these assumptions is purely empirical. A related, but more restricted, effect is demonstrated by the data in Table IX. Here it can be seen that the frequencies of the $-CF_3$ part of the activated complex are little affected by changes in force constants at the reaction center, and also that the additional frequencies present in the activated complex (compared with CF_3) are only slightly dependent on the force constants of $-CF_3$.

Rate constant ratios calculated with Sets TS-I and TS-IIb, differing only in force constants of the $-CF_3$ group, are virtually identical over the temperature range from 333°–1000°K. As discussed above, the same

[32] M. Wolfsberg, "Correction to the Effect of Anharmonicity on Isotopic Exchange Equilibra," Advan. Chem. (to be published).
[33] C. Eckart, Phys. Rev. 35, 1303 (1930).

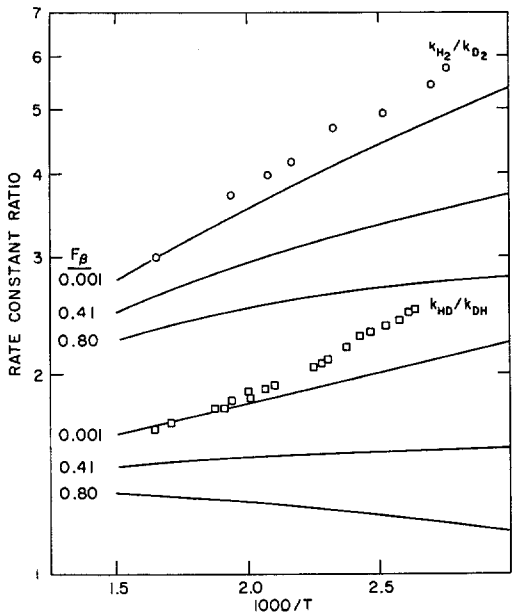

FIG. 6. Effect of F_β on rate constant ratios for a six-atom BEBO model, without tunneling correction (force constant set II).

is true of calculated activation energies. On the other hand, the isotope effects are fairly sensitive to the choice of F_β, since the motion of the H atom being transferred is involved in the coordinate β. This is illustrated in Fig. 6 which shows rate constant ratios as a function of temperature for three different values of F_β. The limiting value of zero for this force constant has the effect of changing the six-atom model back to a three-atom model, since in that case the only coordinates involving the central hydrogen atom are R_{CH}, R_{HH}, and ϕ. Hence, when F_β is 0.001, the predicted isotope effects are essentially those of the three-atom model. The value of 0.41 corresponds to approximately one-half the value in a normal molecule; this is the prescription for determining such bending force constants that has been followed by Johnston and co-workers. The isotope effects predicted with this value are low by 10%–60%, and, particularly in the intramolecular case, the temperature dependence is much too small. This situation is still worse when F_β is 0.80, corresponding to the value for stable molecules.

Analogous results for the cases with tunneling included are shown in Fig. 7. Tunneling corrections were made in the same way as for the three-atom model. Here we find the best agreement given by the largest value of F_β, while the other two values give rate constant ratios which are much too high. With the "prescribed" value of 0.41 for this constant, the tunneling correction increases rate constant ratios so that they are high by 10%–40%. As in the three-atom case, a smaller but nonzero tunneling correction appears necessary, if the bending force constant is fixed at one-half the normal value. However, it is evident that one cannot make a very strong case for the importance of tunneling, unless there is justification for this value of F_β. Similar considerations apply to the work of Sharp and Johnston,[3] where two bending force constants must be assumed: that for ∢F–C–H (as in the present work), and that for ∢H–C–H. However, with tunneling not included in their calculations the isotope effects are too low by as much as a factor of 4; it seems unlikely that this could be corrected by reasonable changes in the bending force constants.

The activation energy predicted from the three-atom model is too low, while that given by the six-atom model with F_β equal to 0.41 is in excellent agreement with the experimental value (Table XI). These energies include the tunneling correction.

Stern and Wolfsberg[34] have discussed the validity of isotope-effect calculations when abbreviated models are used. Their second criterion for "proper cutoff" calculations is that "those changes between reactant and transition state in bond lengths, bond angles, and force constants directly involving the isotopic position(s) must be identical in the complete calculation and the cutoff calculation." Obviously, this condition is not fulfilled by the three-atom model, which lacks one coordinate (β) involving the central hydrogen atom. Thus, one would indeed expect to find differences between the isotope effects predicted from the three-atom and the six-atom models which depend on the particular choice of force constants.

Johnston[35] has suggested that in calculating isotope

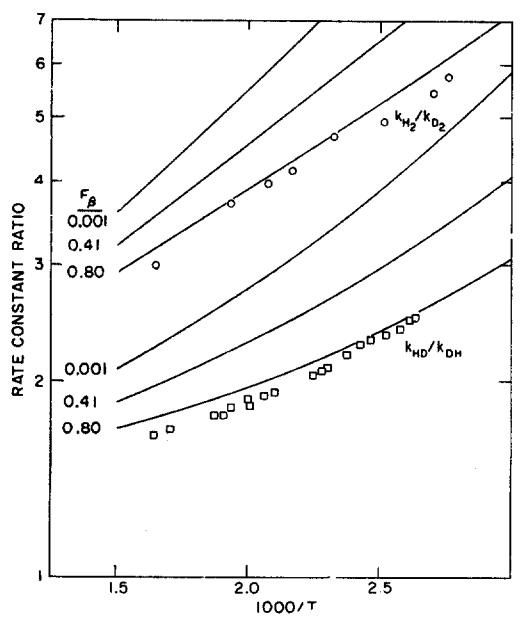

FIG. 7. Effect of F_β on rate constant ratios for a six-atom BEBO model, with one-dimensional tunneling correction (force constant set II).

[34] M. J. Stern and M. Wolfsberg, J. Chem. Phys. **45**, 4105 (1966).

[35] H. S. Johnston, *Gas Phase Reaction Rate Theory* (Ronald Press Co., New York, 1966), p. 346.

effects with the BEBO model, p and q should be set equal and varied to fit the observed activation energy, thus changing the method to a semiempirical one. We have varied $p(=q)$ from 1.05 to 1.10, with a resultant increase in V_a of about 3.5 kcal/mole. Isotope effects calculated without tunneling were virtually identical and much too low with all of these values of p. Tunneling corrections increased with increasing p, and rate constant ratios including this factor were all too high. This approach has the disadvantage of introducing a variable parameter, and at least in this case, does not appear to give better predictions of isotope effects than the original BEBO method, which is completely empirical.

XII. DISCUSSION OF THE LEPS MODEL

The London–Eyring–Polanyi–Sato procedure for obtaining the potential-energy surfaces of triatomic activated complexes has been described in detail elsewhere.[36] This method is semiempirical in that one parameter is adjusted to obtain agreement between a calculated and an experimental value; usually the activation energy has been selected as the criterion. We also followed this procedure, calculating activation energies for a range of values of the parameter κ (formally the square of an overlap integral) which was held equal for each of the two-atom pairs involved. The value of 0.107 gave close agreement of the activation-energy values, which could have been improved with further adjustment of κ. Since the isotope effects are less sensitive to κ than is V_a, further calculation did not seem justified.

The same problem of choosing F_β is present with this model; only the value of 0.41 was tried, but the use of other values should affect rate constant ratios in much the same way as it did in the BEBO calculations. A comparison of the BEBO and LEPS predictions in the absence of tunneling is given by Figs. 6 and 8, and it is seen that the BEBO calculations give significantly better agreement with experiment. Again, the k_{HD}/k_{DH} ratio is very sensitive, and the LEPS calculation gives the wrong sign to the temperature dependence of this ratio.

Two types of tunneling correction were made in calculations with the LEPS model. The first of these used a one-dimensional Eckart barrier in the same way as was done with the BEBO model. Tunneling corrections thus obtained are considerably larger than those of the BEBO model, because of the sharper curvature along the reaction coordinate predicted here. The second type of tunneling correction was that proposed by Johnston and Rapp,[37] which is an attempt to average over a number of one-dimensional barriers. Examination of the potential-energy surface for this reaction in the immediate vicinity of the saddle point indicates that

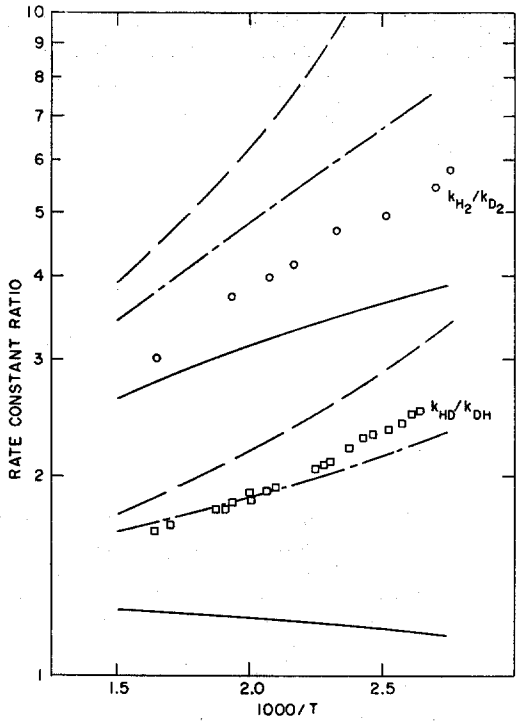

FIG. 8. Isotope effects predicted on the basis of a six-atom LEPS model. —, $\kappa=0.107$, no tunneling (force constant set IIIa); — —, $\kappa=0.107$, one-dimensional tunneling; — – —, $\kappa=0.116$, Johnston–Rapp tunneling (force constant set IIIb).

the reaction path very closely obeys the relationship

$$\Delta R_{CH} = -\Delta R_{HH}.$$

Accordingly, a number of paths parallel to this were used to obtain energy profiles at crossing points near the saddle point. Each of these was then treated as a one-dimensional Eckart barrier, using the appropriate barrier heights and curvature. The resultant tunneling coefficient was then multiplied by a Boltzmann factor which accounts for the increase in barrier height as the reaction path moves away from the saddle point. Finally, these values of the weighted tunneling correction were plotted as a function of the crossing point to obtain the integral over all crossing points.

As Johnston and Rapp pointed out in their original work, this procedure leads to smaller tunneling corrections than does the usual one-dimensional treatment. A slightly different value of 0.116 for κ is necessary in this case to fit the observed activation energy. The one-dimensional treatment gives predicted isotope effects which are much too high (by a factor of 2) whereas the Johnston–Rapp treatment predicts effects which are still too large, but by only 20%–40% (Fig. 8).

XIII. CONCLUSIONS

(1) Reasonable kinetic isotope effects can be predicted from a simplified model for the activated complex. This model uses force constants from empirical or

[36] R. E. Weston, Jr., J. Chem. Phys. **31**, 892 (1959).
[37] H. S. Johnston and D. Rapp, J. Am. Chem. Soc. **83**, 1 (1961).

semiempirical potential-energy surfaces for coordinates around the reaction center, while force constants for other coordinates are taken from stable molecules.

(2) The completely empirical BEBO method predicts isotope effects in this reaction as well as the semiempirical LEPS method.

(3) Because of the uncertainty in the choice of the force constant for the F–C–H bending coordinate, it cannot be asserted that evidence for barrier penetration was found. If the usual value is *assumed* for this force constant, then the results indicate that tunneling must be taking place.

THE JOURNAL OF CHEMICAL PHYSICS VOLUME 49, NUMBER 11 1 DECEMBER 1968

Lifetime of Charged Species in Irradiated Dielectric Liquids

A. HUMMEL

Reactor Institute, Delft, Berlageweg 15, Netherlands

(Received 8 July 1968)

The distribution of lifetimes of the charged species formed in cyclohexane by high-energy radiation is calculated using the experimental results on the number of these species reacting with solutes as a function of the concentration of the solutes. The time in which half of the ions recombine, when no reaction with a solute takes place, is 6×10^{-10} sec. Due to the fact that the diffusion coefficient of the negative entity in cyclohexane at room temperature is very large (2.5×10^{-4} cm^2 sec^{-1}), scavenging of this entity increases the lifetime of the ions considerably. The effect of scavenging of the negative entity on the lifetime distribution is calculated. At large concentrations of α-chlorotoluene the lifetimes of the ions are increased by a factor of 16, approximately. The rate constant for the reaction of the negative entity with α-chlorotoluene at room temperature has been estimated at 4×10^{-11} cm^3 sec^{-1}.

INTRODUCTION

When a fast electron is slowing down in a dielectric liquid, it will suffer losses of a wide range of energies; secondary electrons will be set in motion, which in turn may form tertiaries, and so on. The majority of the losses will be small (<100 eV) and will result in only a few ionizations spaced closely together. Occasionally, a larger energy loss occurs which gives rise to a more extended track of ions. After thermalization or trapping of the electrons, the charge carriers are found in groups, where each ion moves in the field of all the others. The distance between the ions in most groups is such that in dielectric liquids the probability for the ions to escape recombination in the group is small.

In an attempt to obtain information about the spatial distribution of the ions, only the last pair of ions in each group that remains after recombination of all the others has been considered, in this way avoiding the complicated dynamics of a system of more than two charge carriers moving in each other's field. By applying the theory of Onsager on the probability of recombination of an ion pair, the distribution of separations between the ions of the "last pairs" originated by the thermalization of a 1-MeV electron in hexane has been determined.[1]

In principle, it is possible to gain some information about the time scale in which the recombination of the ions in the groups takes place on the basis of our knowledge of the spatial distribution of the ions, provided that the diffusion coefficients of the charge carriers are known. If the probability distribution of the lifetime of an ion pair as a function of the initial separation would be known, the lifetime distribution of the "last ion pairs" originated during the thermalization of a fast electron could be calculated by using the known separations between the pairs. A remaining problem would be to estimate the lifetime distribution of other ion pairs but the "last" ones.

It is possible, however, to obtain information about the lifetime distribution of the charged species in a different way. If the probability of reaction of a charged species with a scavenger molecule during its lifetime is known as a function of the concentration of the scavenger, it is possible to correlate the lifetime distribution of the ions with the yield of scavenged ions as a function of the scavenger concentration. This will now be considered in more detail.[2]

[1] A. Hummel and A. O. Allen, J. Chem. Phys. **44**, 3426 (1966); A. Hummel, A. O. Allen, and F. H. Watson, Jr., *Ibid.* **44**, 3431 (1966); A. Hummel, thesis, Free University, Amsterdam, 1967.

[2] Freeman *et al.*[3] and Williams *et al.*[4] concluded from scavenging experiments that the majority of the charged species recombines within 10^{-11}–10^{-6} sec. They also correlated the lifetime of the ions with the distribution of separations between the last pairs. The lifetime t of a pair of ions of opposite sign as a function of their initial separation r was obtained by considering their movement in each others' Coulomb field, and neglecting diffusion. This leads to the expression $t=(\epsilon/3eu)(r^3-r_0^3)$, where ϵ is the dielectric constant; r_0, the distance at which the recombination reaction takes place; and u, the sum of the mobility of the ions. The values of u they assumed are, however, an order of magnitude smaller than the value we determined in this paper (see also Ref. 5). The separations between the last pairs used by Freeman are also much smaller than the values we determined previously.[1]

[3] G. R. Freeman and J. M. Fayadh, J. Chem. Phys. **43**, 86 (1965); G. R. Freeman, *ibid.* **46**, 2822 (1967).

[4] F. Williams, J. Am. Chem. Soc. **86**, 3954 (1964); J. W. Buchanan and F. Williams, J. Chem. Phys. **44**, 4377 (1966).

[5] S. J. Rzad, R. H. Schuler, and A. Hummel (unpublished).